Spectral Sirens: Cosmology from the Full Mass Distribution of Compact Binaries

Jose María Ezquiaga[1,*] and Daniel E. Holz[1,2]
[1]Kavli Institute for Cosmological Physics and Enrico Fermi Institute, The University of Chicago, Chicago, Illinois 60637, USA
[2]Department of Physics, Department of Astronomy and Astrophysics, The University of Chicago, Chicago, Illinois 60637, USA

(Received 23 February 2022; revised 25 May 2022; accepted 11 July 2022; published 3 August 2022)

We explore the use of the mass spectrum of neutron stars and black holes in gravitational-wave compact binary sources as a cosmological probe. These standard siren sources provide direct measurements of luminosity distance. In addition, features in the mass distribution, such as mass gaps or peaks, will redshift and thus provide independent constraints on their redshift distribution. We argue that the entire mass spectrum should be utilized to provide cosmological constraints. For example, we find that the mass spectrum of LIGO-Virgo-KAGRA events introduces at least five independent mass "features": the upper and lower edges of the pair instability supernova (PISN) gap, the upper and lower edges of the neutron star–black hole gap, and the minimum neutron star mass. We find that although the PISN gap dominates the cosmological inference with current detectors (second generation, 2G), as shown in previous work, it is the lower mass gap that will provide the most powerful constraints in the era of Cosmic Explorer and Einstein Telescope (third generation, 3G). By using the full mass distribution, we demonstrate that degeneracies between mass evolution and cosmological evolution can be broken, unless an astrophysical conspiracy shifts all features of the full mass distribution simultaneously following the (nontrivial) Hubble diagram evolution. We find that this self-calibrating "spectral siren" method has the potential to provide precision constraints of both cosmology and the evolution of the mass distribution, with 2G achieving better than 10% precision on $H(z)$ at $z \lesssim 1$ within a year and 3G reaching $\lesssim 1\%$ at $z \gtrsim 2$ within one month.

DOI: 10.1103/PhysRevLett.129.061102

The expansion rate $H(z)$ is a fundamental observable in cosmology. There has been intense focus on its local value H_0 due to existing $\sim 4\sigma$ tensions between some early and late Universe probes [1,2]. The full redshift distribution of $H(z)$ is also of great interest, since it is a direct probe of the standard cosmological model, Λ cold dark matter (ΛCDM), and may help unveil the nature of dark energy and test general relativity (GR) [3–5]. Compact binary coalescences can be used as standard sirens [6,7]: from the amplitude and frequency evolution of their gravitational-wave (GW) emission, one can directly infer the luminosity distance to the source. This is a particularly powerful probe since it directly measures distance at cosmological scales without any sort of distance ladder, and the sources are calibrated directly by GR. When complemented with electromagnetic counterparts, such as transient events or associated galaxy catalogs, one can infer the redshift and directly constrain cosmological parameters. These bright and dark siren methods have been applied by the LIGO-Virgo Collaborations [8–16], as well as by independent groups [17–20]. Cross-correlations of GWs and galaxy surveys may also constrain $H(z)$ [21–23].

Even in the absence of electromagnetic observations, GWs *alone* can probe $H(z)$ if they are analyzed in conjunction with known astrophysical properties of the population of compact binaries. Cosmology fixes the way in which the observed (redshifted) masses scale with luminosity distance. Therefore, by tracking the mass spectrum in different luminosity distance bins one can infer the redshift of the binaries, transforming them into powerful standard sirens. This "spectral siren" method works best when there is a distinct and easily identifiable feature. Binary neutron stars (BNSs) were the first to be proposed due to the expected maximum upper limit on the mass of neutron stars [24,25]. The masses of binary black holes (BBHs) also show interesting features, including a pronounced dearth of BBHs at high mass [26,27]. This feature is thought to come from the theory of pair instability supernova (PISN) [28–33], which robustly predicts a gap between ~ 50 and 120 $M_\odot$. The lower edge of the PISN gap is a clear target for second-generation (2G) detectors [34] and has been explored for third-generation (3G) interferometers [35]. Constraints on H_0 from the latest catalog are $\sim 20\%$ at 1σ [15]. Second-generation detectors at A+ sensitivity and 3G could also detect far-side black holes on the other side of the gap, thereby resolving the upper edge of the PISN gap and providing another anchor for cosmography [36].

We explore the capabilities of current and next-generation detectors to probe $H(z)$ with the *full* mass distribution of compact binaries. Uncertainties in the astrophysical modeling of the mass spectrum [37,38] can impact the cosmological inference. We focus on the possible biases induced by the evolution of the masses and demonstrate that these degeneracies can be broken with

spectral sirens. By using the entire mass distribution, the population itself allows one to constrain potential systematics due to evolution—in this sense, spectral sirens are *self-calibrating*. We concentrate on flat ΛCDM, but our methods can be straightforwardly generalized to other models. Our method can also be used to test GR [39], as demonstrated with current BBH data [39–41], and could be extended to BNSs [42,43]. Measuring tidal effects in BNS will provide additional redshift information given the universality of the equation of state of matter at nuclear density [44,45].

Five independent probes of cosmology.—Our understanding of the population of stellar-origin compact binaries is far from complete. However, current GWs catalogs already provide suggestive and interesting insights [27,46,47]. In this Letter, we focus on the mass distribution, for which a number of broad properties are already well constrained: (i) A drop in the BBH rate above $\sim 45\ M_\odot$: This dearth of mergers of more massive BBHs is statistically robust and coincides with the range of masses where LIGO-Virgo are most sensitive [26,27,36]. Data suggest that this feature can be modeled with a broken power law. (ii) A drop in the rate at $\sim 2.5\ M_\odot$ and a break at $\sim 5\ M_\odot$ in the power law behavior above this mass [27,48]: The sharp feature at $\sim 2.5\ M_\odot$ is statistically well resolved and robust, but data are inconclusive as to the distribution within the putative gap at ~ 2.5–$5\ M_\odot$. Overall, the most likely local rate of binaries with component masses below $\sim 2.5\ M_\odot$ is about 10 times larger than the rate above $\sim 5\ M_\odot$, although uncertainties are still large [27]. Interestingly, the evidence of (i) is roughly consistent with the prediction for a "PISN gap" or "upper mass gap." Since current sensitivities drop above the upper edge of the PISN gap, we are still agnostic about a possible population of "far-side binaries" above this feature [36], although we have upper bounds on their rate [49]. On the other hand, (ii) would be consistent with electromagnetic observations suggesting a "neutron star black hole gap" or "lower mass gap" [50–52]. GW data robustly suggest that both BNSs and BBHs cannot be described by a single power law, but it cannot conclusively resolve the precise nature of the gap [48]. Subsolar mass astrophysical binaries are currently disfavored by theory, since objects more compact than white dwarfs are not expected as the end point of stellar evolution in this mass range [53]. Furthermore, they are disfavored by data, as targeted searches have found no candidates [54].

The evidence for these features in the mass distribution of compact binaries suggests that there will be at least five independent mass scales: the edges of the lower and upper mass gaps, as well as the minimum neutron star mass. Each of these scales can be used to anchor the mass distribution in the *source* frame, and thus the *detector*-frame distributions will allow us to infer the redshift,

$$z(d_L) = m^{\rm det}_{\rm edge}(d_L)/m_{\rm edge} - 1, \tag{1}$$

where $m_{\rm edge} = m^{\rm det}_{\rm edge}(d_L = 0)$. Our fiducial, toy-model population is composed of a uniform distribution of BNSs between 1 and 2.5 $M_\odot$, a broken power law model for BBHs below the PISN gap between a minimum and maximum mass, and a uniform distribution of far-side binaries. The local rates are fixed to $\mathcal{R}_0^{\rm BNS} = 320$, $\mathcal{R}_0^{\rm BBH} = 30$, and $\mathcal{R}_0^{\rm far-side} = 0.1\ {\rm Gpc}^{-3}\ {\rm yr}^{-1}$, respectively, being consistent with population analyses [27] and upper limits on intermediate-mass black holes [49]—see Supplemental Material for technical details [55], which includes Refs. [56–62]. Although 2G instruments detect a greater fraction of high-mass sources due to selection effects, 3G instruments are expected to detect *all* sources and will be equally sensitive to BNSs and BBHs across the mass spectrum. We assume the merger rates follow the star formation rate [63].

The real distribution of compact binaries will certainly be more complex than the above description. Additional features will be beneficial, since these will introduce extra reference scales that can be tracked in the same way as the edges of the mass gaps, for example, the current excess of detections at $\sim 35\ M_\odot$ [27]. Moreover, since edges are easier to find than peaks, the cosmological inference will be dominated by the gaps. The utility of these features will be related to their prominence, such as the sharpness of the edges. For simplicity, we consider the gap edges to be step functions—more detailed calculations with smooth transitions provide constraints at the same order of magnitude, see, e.g., [34].

The lower mass gap will win.—The constraints on $H(z)$ are most sensitive to how well we resolve the edges of the mass gaps, which is directly related to the number of events at these scales at different redshifts. These numbers will be a combination of the detector sensitivity and the intrinsic merger rate $\mathcal{R}(z)$. Despite the larger intrinsic rate of low-mass binaries, the selection effects of 2G detectors significantly reduces the detectability. This changes with 3G detectors [64], where essentially all astrophysical stellar-origin binaries are detected across cosmic history. Quantitatively, for 2G detectors we find ∼6% of detections having masses below 7 $M_\odot$ and ∼10% above 45 $M_\odot$. With 3G sensitivities, these numbers shift to ∼27% below 7 $M_\odot$ and ∼2% above 45 $M_\odot$. This suggests that the lower mass gap will play an increasingly important role transitioning to 3G.

The precision in $H(z)$ depends on the errors in distance and redshift. The error in d_L scales as $1/\sqrt{N}$, where N is the relevant number of binaries providing the measurement (see, e.g., [65,66]). The error on the redshift is dominated by the uncertainty in locating features in the observed mass distribution. For example, the error in locating the "edge" of a mass gap is expected to scale as $1/N$ [36], so long as the errors in the individual mass measurements are subdominant. Since, generally, distance is measured more poorly than mass, we find

$$\frac{\Delta H(z)}{H(z)} \sim \frac{\Delta d_L/d_L}{\sqrt{N_{\rm edge}}}, \tag{2}$$

where $N_{\rm edge}$ is the number of events with information about the edge. We follow [67] to simulate GW detections including selection effects and detector uncertainties. Dividing the number of detections into four redshift bins for $z < 2$, we estimate $\Delta H(z)/H(z)$ from each edge of the mass gaps.

Although the lower edge of the PISN mass gap will dominate the inference of $H(z)$ with current detectors (reaching 5%–10%, in agreement with [34]), it is the lower mass gap that will dominate the 3G inference, potentially reaching subpercent precision. Moreover, with 3G detectors the precision in $H(z)$ is sustained beyond $z > 1$.

Degeneracies between cosmology and mass evolution can be broken.—For spectral sirens, it is critical to understand if the mass distribution itself evolves, since such evolution might bias the inference of $H(z) = H_0\sqrt{\Omega_m(1+z)^3+1-\Omega_m}$, where H_0 and Ω_m are the expansion rate and (dimensionless) matter density today. For convenience, we also introduce $h_0 = H_0/(100\ \mathrm{km/s/Mpc})$.

In the context of 3G, and assuming $\mathcal{R}(z)$ peaks around $z \sim 2$, the vast majority of binaries will be detected for all viable ranges of cosmological parameters [68]. We can therefore neglect any mass or redshift dependence in the detection probability, and the effect of modifying cosmology becomes transparent: (a) it changes the overall rate as a function of redshift, and (b) it shifts the detector frame masses of the entire population. For $\mathcal{R}(z)$ following the star formation rate, there is no clear correlation with (H_0, Ω_m), except for the degeneracy between $\mathcal{R}_0$ and H_0^3. Importantly, the bulk of the cosmological constraints will come from the observed mass distribution rather than the overall rate.

The evolution of the mass distribution does not mimic the cosmology unless the *entire* spectrum shifts uniformly, so that the shape is completely unaltered. However, in general, we would expect the evolution to change its shape, see, e.g., [69,70], and therefore, cosmology and evolution of the mass distribution can be disentangled. Nonetheless, we can imagine that time evolution might affect one of the edges of one of our mass bins. As an example, we consider a linear-in-redshift mass evolution controlled by γ, i.e., $m_{\rm edge,ev}(z) = m_{\rm edge} + \gamma z$, assuming that $m_{\rm edge}$ is measured at $z \sim 0$. In this case, the inferred redshift when not taking this evolution into account will be biased by

$$z_{\rm bias} = (1+z)(1+\gamma z/m_{\rm edge}) - 1. \tag{3}$$

Consequently, if $\gamma > 0$, $z_{\rm bias}$ will be shifted toward higher values which, at fixed d_L, is equivalent to a larger H_0. For example, a 0.1 $M_\odot$ shift of a 5 $M_\odot$ edge at $z \sim 1$ will change $H(z)$ by ∼3%. Importantly, this is only an approximate degeneracy. As shown in Fig. 1, when considering the Hubble diagram at all redshifts, the effect of astrophysical evolution will not, in general, match with any allowable ΛCDM cosmologies. An evolution of the mass scale that mimics the low-z effect of changing h_0 will overshoot the modification of Ω_m at high z. Because the larger differences occur at $z > 1$, this figure helps us anticipate that 3G detectors will more effectively disentangle the astrophysical evolution from varying cosmology. Note that, although we have chosen a particular parametrization for $m_{\rm edge,ev}(z)$, our conclusions hold, in general: we can disentangle evolution of the mass distribution so long as it is not perfectly tuned to change in accordance with the (highly nontrivial) Hubble diagram shown in Fig. 1 at all mass scales.

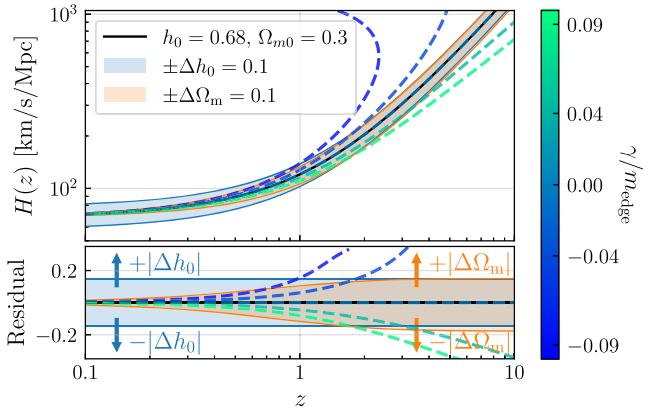

FIG. 1. Inferred Hubble parameter for different fiducial cosmologies (color bands) and evolutions of an edge of the mass distribution (dashed lines). We assume that $m_{\rm edge}$ is measured at low redshift and the redshift is biased by the linear evolution γ, cf. (3). Bottom: corresponds to the residual against the fiducial cosmology $[H(z) - H_{\rm fid}(z)]/H_{\rm fid}(z)$, with $H_{\rm fid}(z)$ fixed by $h_0 = 0.68$ and $\Omega_m = 0.3$ (black line). Arrows indicate the effect of changing h_0 and Ω_m.

Examples of 2G and 3G inference.—To explore the degeneracy space between different cosmologies and astrophysical evolution, we generate a mock catalog of events and perform a Bayesian hierarchical analysis to infer $H(z)$. In particular, we study how the inference of (h_0, Ω_m) is affected by the fiducial population model. We focus on BBHs between the lower and upper mass gaps, delimited by $m_{\rm min}$ and $m_{\rm max}$, considering three scenarios: (1) no evolution: the intrinsic population has fixed edges over cosmic time ($\gamma_{\rm min} = \gamma_{\rm max} = 0\ M_\odot$), (2) one-sided evolution: the maximum mass increases with redshift ($\gamma_{\rm min} = 0\ M_\odot$, $\gamma_{\rm max} \neq 0\ M_\odot$), (3) independent two-sided evolution: both the minimum and maximum masses evolve ($\gamma_{\rm min}, \gamma_{\rm max} \neq 0\ M_\odot$). We consider 1000 2G detections at A + sensitivity [71,72], and 10 000 3G events at Cosmic Explorer sensitivity [73]. This corresponds to roughly 1 yr and 1 month of observation, respectively. For simplicity, we restrict the Bayesian inference to the most relevant parameters: $\{h_0, \Omega_m, m_{\rm min}, m_{\rm max}, \gamma_{\rm min}, \gamma_{\rm max}\}$; we have checked explicitly that this assumption does not affect our

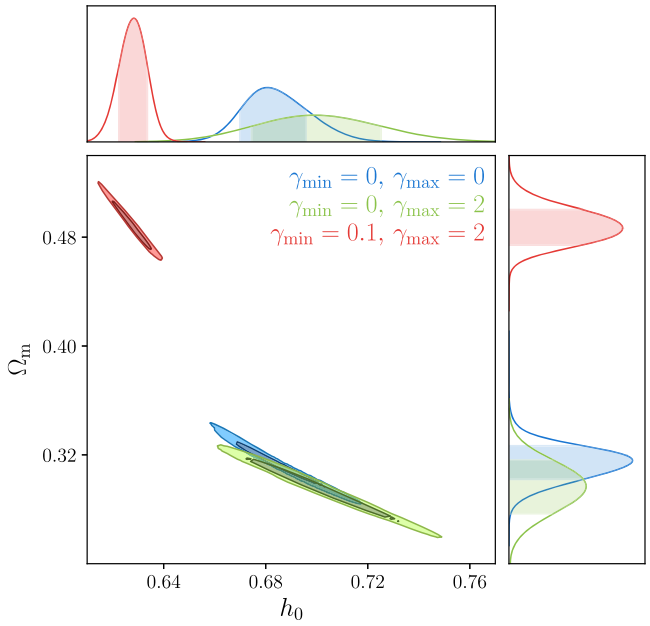

FIG. 2. Cosmological inference with 10 000 3G BBH detections between fixed lower and upper mass gaps, when the fitting model does *not* include evolution in the mass distribution. Different posterior distributions correspond to three mock populations: without evolution (blue), with evolution of the maximum mass (green), and evolution of both minimum and maximum masses (red). When not accounted for, the evolution of the mass distribution can bias h_0 and Ω_m.

conclusions. Full posterior samples can be found in the Supplemental Material [55].

We first analyze how the cosmological inference changes for different mock populations when the potential evolution of the mass distribution is not incorporated in the parameter estimation. When the mock catalog does not evolve, the fiducial cosmological parameters are well recovered since the fitting model matches the simulated data. However, when the catalogs include evolution, the inference of (h_0, Ω_m) can become biased. This is especially acute for 3G, as plotted in Fig. 2. In this case, the larger bias occurs for the case of an evolving minimum mass ($\gamma_{\rm min} \neq 0$, red posteriors), since this is the scale controlling the inference. The red contours show that, since the minimum mass is increasing with redshift, the inferred redshifts are biased high, and thus to compensate h_0 is biased to lower values and Ω_m is biased to higher values (see Fig. 1). In the case where the minimum mass does not evolve while the maximum mass does evolve (green contours), the cosmology is not biased significantly, but the errors enlarge as the inference from the upper mass is degraded.

We also analyze the same mock catalogs including $\gamma_{\rm min}$ and $\gamma_{\rm max}$ as free parameters. We find that h_0 and Ω_m are no longer biased, although Ω_m is now poorly constrained with 2G detectors in agreement with [37], with the evolution parameters recovered at $\Delta\gamma_{\rm min}/\gamma_{\rm min} \sim 20\%$ and $\Delta\gamma_{\rm max}/\gamma_{\rm max} \sim 8\%$. 3G places significantly better constraints with more accuracy at low masses, $\Delta\gamma_{\rm min}/\gamma_{\rm min} \sim 1\%$ and $\Delta\gamma_{\rm max}/\gamma_{\rm max} \sim 3\%$.

These results indicate that both 2G and 3G detectors will be able to simultaneously constrain cosmology and measure the evolution of the mass distribution. Translated into a measurement of the expansion rate (at 68% C.L.), 2G detectors will within a year constrain $H(z)$ with better than 10% accuracy at $z \sim 0.7$. This result is slightly inferior to the previous ~6% forecast of $H(z \sim 0.8)$ in one year from the PISN mass gap [34]. This is because we adopt the latest fit to the data, consisting of a broken power law with a less pronounced lower edge of the gap [27]. A similar conclusion was found in [37]. Impressively, 3G detectors will within a month constrain $H(z)$ with $< 1\%$ accuracy beyond $z \sim 1$, comparing favorably to measurements such as DESI [74] as shown in Fig. 3. Although our modeling of the mass distribution is only a rough parametrization, it provides a useful estimate of the capabilities of future detectors. We leave a detailed cosmological forecast with realistic BBH mass distributions from different formation channels for future work.

Future prospects.—Next-generation GW detectors will perform subpercent precision cosmography with standard sirens, providing a potentially revolutionary new cosmological probe. A detailed understanding of the attendant systematics will be required to attain robust constraints. We have shown that in the 3G era the spectral siren measurement of $H(z)$ will be dominated by features associated with the lower mass gap. Moreover, by incorporating the possibility of redshift evolution of the intrinsic mass distribution, it is possible to simultaneously constrain such evolution along with the underlying cosmological model.

We emphasize the utility of using the full mass distribution, rather than focusing on just one feature such as the lower edge of the upper or PISN mass gap. Each of the edges of the mass gaps (or any other relevant feature) can be thought of as providing an independent cosmological measurement. One can compare the values of H_0 and Ω_m from each individual bump and wiggle and dip in the mass distribution, and in this way the GW population is self-calibrating: it can simultaneously constrain cosmology while testing for consistency and unearthing systematics due to population evolution. Alternatively, a Bayesian analysis of the entire catalog helps to narrow down the errors in $H(z)$ and simultaneously constrain the astrophysical evolution of the mass distribution. This work considers a simple, toy-model description for the mass distribution. In practice, the spectral siren method will utilize the full data-informed mass distribution incorporating all of the identifiable features simultaneously. The results can be thought of as a conservative estimate of the future potential of this approach and have implications both for cosmology and for our understanding of the formation and evolution of the relevant astrophysical populations.

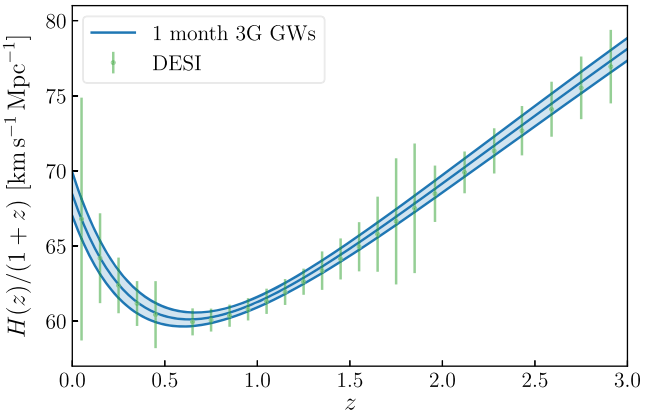

FIG. 3. Hubble parameter with 10 000 3G detections when the fitting model *does* account for evolution in the mass distribution. Shaded region represents 1σ errors. Subpercent precision is possible with 1 month of observation. We compare to DESI forecasts [74].

One of the outstanding challenges of GW astrophysics is to develop an understanding of the formation channels that account for GW observations (see, e.g., [75,76]). Recent work has explored the evolution of the mass distribution in field binaries [69] and clusters [70,77], and searches have been performed in current data [78]. These works show that the high-mass end of the distribution is more susceptible to environmental effects, such as metallicity, that are expected to evolve with cosmic time, as well as the time delay distribution that affects the observed relative rates [38,69]. It is encouraging that current results indicate that the low-mass end of the spectrum could be more robust against redshift evolution, while providing the strongest constraints on $H(z)$. Given the potential scientific impact of the lower mass gap for cosmology, further exploration of its properties is warranted. Moreover, although other quantities such as mass ratios and spins do not redshift, if their intrinsic distributions evolve in time in a known fashion, they could provide redshift information as a spectral siren.

Since spectral siren cosmology is a pure GW measurement, it is completely independent from results based on electromagnetic observations. We have shown that the GW constraints compare favorably with current ~6%–10% baryon acoustic oscillation constraints from BOSS [79–81] and future forecasts, such as the $> 2\%$ measurements expected from DESI [74] at $H(z > 2)$. The spectral siren method is complementary to the bright siren approach, which uses electromagnetic counterparts to GW sources to constrain the redshift of the sources [6,7,65]. For ground-based detectors, the most promising counterpart sources are short gamma-ray bursts associated with BNSs. While these may be detectable to $z \gtrsim 0.5$, they are likely inaccessible at $z \gtrsim 1.5$ [82,83]. Thus, spectral sirens will provide unique precision high-redshift constraints on both GW astrophysics and cosmology.

We are grateful to Amanda Farah, Will Farr, and Mike Zevin for stimulating conversations. We also thank Amanda Farah, and Rachel Gray for comments on the draft, and Antonella Palmese and Aaron Tohuvavohu for useful correspondence. J. M. E. is supported by NASA through the NASA Hubble Fellowship Grant No. HST-HF2-51435.001-A awarded by the Space Telescope Science Institute, which is operated by the Association of Universities for Research in Astronomy, Inc., for NASA, under Contract No. NAS5-26555. D. E. H. is supported by NSF Grants No. PHY-2006645 and No. PHY-2110507. D. E. H. also gratefully acknowledges support from the Marion and Stuart Rice Award. Both authors are also supported by the Kavli Institute for Cosmological Physics through an endowment from the Kavli Foundation and its founder Fred Kavli.

*ezquiaga@uchicago.edu

[1] W. L. Freedman, Nat. Astron. **1**, 0121 (2017).
[2] L. Verde, T. Treu, and A. G. Riess, Nat. Astron. **3**, 891 (2019).
[3] J. Frieman, M. Turner, and D. Huterer, Annu. Rev. Astron. Astrophys. **46**, 385 (2008).
[4] T. Clifton, P. G. Ferreira, A. Padilla, and C. Skordis, Phys. Rep. **513**, 1 (2012).
[5] J. M. Ezquiaga and M. Zumalacárregui, Front. Astron. Space Sci. **5**, 44 (2018).
[6] B. F. Schutz, Nature (London) **323**, 310 (1986).
[7] D. E. Holz and S. A. Hughes, Astrophys. J. **629**, 15 (2005).
[8] J. Aasi *et al.*, Classical Quantum Gravity **32**, 115012 (2015).
[9] F. Acernese *et al.*, Classical Quantum Gravity **32**, 024001 (2015).
[10] B. P. Abbott *et al.* (LIGO Scientific, Virgo, 1M2H, Dark Energy Camera GW-E, DES, DLT40, Las Cumbres Observatory, VINROUGE, MASTER Collaboration), Nature (London) **551**, 425 (2017).
[11] M. Fishbach *et al.* (LIGO Scientific, Virgo Collaborations), Astrophys. J. Lett. **871**, L13 (2019).
[12] M. Soares-Santos *et al.* (DES, LIGO Scientific, Virgo Collaborations), Astrophys. J. Lett. **876**, L7 (2019).
[13] R. Abbott *et al.* (LIGO Scientific, Virgo Collaborations), Astrophys. J. Lett. **896**, L44 (2020).
[14] B. P. Abbott *et al.* (LIGO Scientific, Virgo Collaborations), Astrophys. J. **909**, 218 (2021); **923**, 279(E) (2021).
[15] R. Abbott *et al.* (LIGO Scientific, Virgo, KAGRA Collaborations), arXiv:2111.03604.
[16] A. Palmese *et al.* (DES Collaborations), Astrophys. J. Lett. **900**, L33 (2020).
[17] S. Vasylyev and A. Filippenko, Astrophys. J. **902**, 149 (2020).
[18] A. Finke, S. Foffa, F. Iacovelli, M. Maggiore, and M. Mancarella, J. Cosmol. Astropart. Phys. 08 (2021) 026.
[19] A. Palmese, C. R. Bom, S. Mucesh, and W. G. Hartley, arXiv:2111.06445.
[20] R. Gray, C. Messenger, and J. Veitch, Mon. Not. R. Astron. Soc. **512**, 1127 (2022).
[21] M. Oguri, Phys. Rev. D **93**, 083511 (2016).
[22] S. Mukherjee, B. D. Wandelt, S. M. Nissanke, and A. Silvestri, Phys. Rev. D **103**, 043520 (2021).

[23] C. C. Diaz and S. Mukherjee, Mon. Not. R. Astron. Soc. **511**, 4377 (2022).
[24] D. F. Chernoff and L. S. Finn, Astrophys. J. Lett. **411**, L5 (1993).
[25] S. R. Taylor, J. R. Gair, and I. Mandel, Phys. Rev. D **85**, 023535 (2012).
[26] M. Fishbach and D. E. Holz, Astrophys. J. Lett. **851**, L25 (2017).
[27] R. Abbott *et al.* (LIGO Scientific, Virgo, KAGRA Scientific Collaborations), arXiv:2111.03634.
[28] Z. Barkat, G. Rakavy, and N. Sack, Phys. Rev. Lett. **18**, 379 (1967).
[29] W. A. Fowler and F. Hoyle, Astrophys. J. Suppl. Ser. **9**, 201 (1964).
[30] A. Heger and S. E. Woosley, Astrophys. J. **567**, 532 (2002).
[31] C. L. Fryer, S. E. Woosley, and A. Heger, Astrophys. J. **550**, 372 (2001).
[32] A. Heger, C. L. Fryer, S. E. Woosley, N. Langer, and D. H. Hartmann, Astrophys. J. **591**, 288 (2003).
[33] K. Belczynski, A. Heger, W. Gladysz, A. J. Ruiter, S. Woosley, G. Wiktorowicz, H. Y. Chen, T. Bulik, R. O'Shaughnessy, D. E. Holz, C. L. Fryer, and E. Berti, Astron. Astrophys. **594**, A97 (2016).
[34] W. M. Farr, M. Fishbach, J. Ye, and D. Holz, Astrophys. J. Lett. **883**, L42 (2019).
[35] Z.-Q. You, X.-J. Zhu, G. Ashton, E. Thrane, and Z.-H. Zhu, Astrophys. J. **908**, 215 (2021).
[36] J. M. Ezquiaga and D. E. Holz, Astrophys. J. Lett. **909**, L23 (2021).
[37] S. Mastrogiovanni, K. Leyde, C. Karathanasis, E. Chassande-Mottin, D. A. Steer, J. Gair, A. Ghosh, R. Gray, S. Mukherjee, and S. Rinaldi, Phys. Rev. D **104**, 062009 (2021).
[38] S. Mukherjee, arXiv:2112.10256.
[39] J. M. Ezquiaga, Phys. Lett. B **822**, 136665 (2021).
[40] M. Mancarella, E. Genoud-Prachex, and M. Maggiore, Phys. Rev. D **105**, 064030 (2022).
[41] K. Leyde, S. Mastrogiovanni, D. A. Steer, E. Chassande-Mottin, and C. Karathanasis, arXiv:2202.00025.
[42] C. Ye and M. Fishbach, Phys. Rev. D **104**, 043507 (2021).
[43] A. Finke, S. Foffa, F. Iacovelli, M. Maggiore, and M. Mancarella, Phys. Dark Universe **36**, 100994 (2022).
[44] C. Messenger and J. Read, Phys. Rev. Lett. **108**, 091101 (2012).
[45] D. Chatterjee, A. Hegade K. R., G. Holder, D. E. Holz, S. Perkins, K. Yagi, and N. Yunes, Phys. Rev. D **104**, 083528 (2021).
[46] B. P. Abbott *et al.* (LIGO Scientific, Virgo Collaborations), Astrophys. J. Lett. **882**, L24 (2019).
[47] R. Abbott *et al.* (LIGO Scientific, Virgo Collaborations), Astrophys. J. Lett. **913**, L7 (2021).
[48] A. M. Farah, M. Fishbach, R. Essick, D. E. Holz, and S. Galaudage, Astrophys. J. **931**, 108 (2022).
[49] R. Abbott *et al.* (LIGO Scientific, Virgo, KAGRA Collaborations), Astron. Astrophys. **659**, A84 (2022).
[50] C. D. Bailyn, R. K. Jain, P. Coppi, and J. A. Orosz, Astrophys. J. **499**, 367 (1998).
[51] F. Ozel, D. Psaltis, R. Narayan, and J. E. McClintock, Astrophys. J. **725**, 1918 (2010).
[52] W. M. Farr, N. Sravan, A. Cantrell, L. Kreidberg, C. D. Bailyn, I. Mandel, and V. Kalogera, Astrophys. J. **741**, 103 (2011).
[53] S. Chandrasekhar, Astrophys. J. **74**, 81 (1931).
[54] R. Abbott *et al.* (LIGO Scientific, Virgo, KAGRA Collaborations), arXiv:2109.12197.
[55] See Supplemental Material at http://link.aps.org/supplemental/10.1103/PhysRevLett.129.061102 for a detailed description of the methodology, population prior specifications and full posterior samples.
[56] A. Nitz *et al.*, GWASTRO/PyCBC: PyCBC release v1.14.4 (2019).
[57] S. Husa, S. Khan, M. Hannam, M. Pürrer, F. Ohme, X. J. Forteza, and A. Bohé, Phys. Rev. D **93**, 044006 (2016).
[58] I. Mandel, W. M. Farr, and J. R. Gair, Mon. Not. R. Astron. Soc. **486**, 1086 (2019).
[59] W. M. Farr, Res. Notes AAS **3**, 66 (2019).
[60] T. Callister, M. Fishbach, D. Holz, and W. Farr, Astrophys. J. Lett. **896**, L32 (2020).
[61] D. Foreman-Mackey, D. W. Hogg, D. Lang, and J. Goodman, Publ. Astron. Soc. Pac. **125**, 306 (2013).
[62] S. R. Hinton, J. Open Source Software **1**, 45 (2016).
[63] P. Madau and M. Dickinson, Annu. Rev. Astron. Astrophys. **52**, 415 (2014).
[64] S. Vitale, Phys. Rev. D **94**, 121501(R) (2016).
[65] N. Dalal, D. E. Holz, S. A. Hughes, and B. Jain, Phys. Rev. D **74**, 063006 (2006).
[66] H.-Y. Chen, M. Fishbach, and D. E. Holz, Nature (London) **562**, 545 (2018).
[67] M. Fishbach, W. M. Farr, and D. E. Holz, Astrophys. J. Lett. **891**, L31 (2020).
[68] N. Aghanim *et al.* (Planck Collaboration), Astron. Astrophys. **641**, A6 (2020); **652**, C4(E) (2021).
[69] L. A. C. van Son, S. E. de Mink, T. Callister, S. Justham, M. Renzo, T. Wagg, F. S. Broekgaarden, F. Kummer, R. Pakmor, and I. Mandel, Astrophys. J. **931**, 17 (2022).
[70] M. Mapelli, Y. Bouffanais, F. Santoliquido, M. A. Sedda, and M. C. Artale, Mon. Not. R. Astron. Soc. **511**, 5797 (2022).
[71] B. P. Abbott *et al.* (KAGRA, LIGO Scientific, Virgo Collaborations), Living Rev. Relativity **21**, 3 (2018).
[72] L.V.K. Collaboration, Ligo sensitivity curves, https://dcc.ligo.org/LIGO-T2000012/public.
[73] M. Evans, R. Sturani, S. Vitale, and E. Hall, 3g sensitivity curves, https://dcc.ligo.org/LIGO-T1500293-v11/public.
[74] A. Aghamousa *et al.* (DESI Collaborations), arXiv:1611.00036.
[75] M. Zevin, S. S. Bavera, C. P. L. Berry, V. Kalogera, T. Fragos, P. Marchant, C. L. Rodriguez, F. Antonini, D. E. Holz, and C. Pankow, Astrophys. J. **910**, 152 (2021).
[76] I. Mandel and F. S. Broekgaarden, Living Rev. Relativity **25**, 1 (2022).
[77] M. Zevin and D. E. Holz, arXiv:2205.08549.
[78] M. Fishbach, Z. Doctor, T. Callister, B. Edelman, J. Ye, R. Essick, W. M. Farr, B. Farr, and D. E. Holz, Astrophys. J. **912**, 98 (2021).
[79] H. du Mas des Bourboux *et al.*, Astron. Astrophys. **608**, A130 (2017).
[80] J. E. Bautista *et al.*, Astron. Astrophys. **603**, A12 (2017).
[81] P. Zarrouk *et al.*, Mon. Not. R. Astron. Soc. **477**, 1639 (2018).
[82] E. Belgacem, Y. Dirian, S. Foffa, E. J. Howell, M. Maggiore, and T. Regimbau, J. Cosmol. Astropart. Phys. 08 (2019) 015.
[83] H.-Y. Chen, P. S. Cowperthwaite, B. D. Metzger, and E. Berger, Astrophys. J. Lett. **908**, L4 (2021).